
NON-SEQUENTIAL ENSEMBLE KALMAN FILTERING USING DISTRIBUTED ARRAYS

Cédric Travelletti^{*1,2,4}, Jörg Franke^{†3,4}, David Ginsbourger^{2,3}, and Stefan Brönnimann^{3,4}

¹Mathematics for Materials Modelling, Institute of Mathematics & Institute of Materials, EPFL, Lausanne, Switzerland

²Institute of Mathematical Statistics and Actuarial Science, University of Bern, Bern, Switzerland

³Oeschger Center for Climate Change Research, University of Bern, Bern, Switzerland

⁴Institute of Geography, University of Bern, Bern, Switzerland

November 23, 2023

ABSTRACT

This work introduces a new, distributed implementation of the Ensemble Kalman Filter (EnKF) that allows for non-sequential assimilation of large datasets in high-dimensional problems. The traditional EnKF algorithm is computationally intensive and exhibits difficulties in applications requiring interaction with the background covariance matrix, prompting the use of methods like sequential assimilation which can introduce unwanted consequences, such as dependency on observation ordering. Our implementation leverages recent advancements in distributed computing to enable the construction and use of the full model error covariance matrix in distributed memory, allowing for single-batch assimilation of all observations and eliminating order dependencies. Comparative performance assessments, involving both synthetic and real-world paleoclimatic reconstruction applications, indicate that the new, non-sequential implementation outperforms the traditional, sequential one.

*cedric.travelletti@unibe.ch

†joerg.franke@unibe.ch

1 Introduction

Kalman filtering is a data assimilation method that aims at estimating the state of a dynamic system from a series of measurements. It has been used successfully in a variety of domains such as aerospace engineering, robotics, navigation systems, financial economics and climate science. In spite of these achievements, the original Kalman filter suffers from several limitations that prevent its application at larger scales. This has given rise to a variety of modified Kalman filters, such as the Extended Kalman Filter (EKF) [16, 31], the Unscented Kalman Filter (UKF) [27, 44] and the Ensemble Kalman Filter (EnKF) [10]. Of all the computational difficulties associated with the standard Kalman filter, most of them can be traced back to the background covariance matrix. Indeed, this matrix is quadratic in the number of prediction points, which makes it hard to handle and store at larger problem sizes. One approach proposed to alleviate these difficulties is the ensemble Kalman filter (EnKF), first introduced by [10] and subsequently developed in [11, 12]. Ensemble Kalman filtering gets rid of the background covariance matrix by instead updating sequentially a sample (ensemble) of the prior background distribution and using the empirical sample covariance as an approximation of the true covariance. Thus, instead of storing a full covariance matrix, EnKF only has to store the (updated) ensemble members at each step.

For most applications, the EnKF provides an efficient, tractable approximation to the standard Kalman filter, but it has one significant drawback: for any application that requires interfering with the covariance, the difficulties of the standard Kalman filter reappear. An example of such an application is covariance regularization. Indeed, at tractable (small) ensemble sizes, the empirical covariance suffers from undersampling, which significantly degrades the performance of the filter due to spurious long-range correlations, variance underestimation, artifacts and other estimation errors. This means that, in practice, the empirical covariance has to be regularized before it can be used for filtering [1, 22], hence requiring access to the full matrix, bringing us back to the chores of the original filter.

In practice, these problems are usually solved by considering some sequential version of the filter [24], where observations are assimilated in batches, so that, at each iteration, only the parts of the covariance associated to the data points being currently assimilated need to be computed. It has long been known in the data assimilation community that, when used in conjunction with covariance regularization techniques, sequential processing breaks down the theoretical guarantees of the EnKF and can yield unwanted consequences. These include, among others, dependency of the results on observations ordering. Heuristical approaches for "optimal" observation ordering during assimilation have been proposed [48], and while the problem is known, practical applications of the EnKF resort to sequential assimilation as a last resort, owing to the computational impossibility of assimilating all data synchronously, as would be required by the original filter formulation.

The first, and to our knowledge only, systematic study of order dependency in sequential ensemble Kalman filtering was undertaken by [34]. This study demonstrates that the use of covariance localization [22] leads to observation ordering dependency when used in the square root ensemble Kalman filter of [41]. The study concludes that when observational errors are similar in magnitude to model errors, the ordering effect is of moderate significance. While such an assumption can be met in some setups, it does not hold in general for ensemble-based climate reconstructions [2] where model uncertainties can be large.

In this work, we introduce a new implementation of the ensemble Kalman filter that leverages the most recent progress in distributed computing. Through the use of distributed arrays [8, 37], the full model error covariance matrix can be built in (distributed) memory, which allows our implementation to assimilate all observations in a single batch (all-at-once), thus getting rid of ordering dependencies. This allows to use localization in EnKF while still retaining the theoretical properties of the original filter. The computational scalability of this new implementation allows it to conduct all-at-once, localized, EnKF assimilation on large-scale problems such as global climate reconstruction [2, 6, 39, 14]. We believe that by leveraging the most recent developments in distributed computing, this new approach opens the door to a principled use of covariance localization in large-scale applications of ensemble (square-root) Kalman filtering.

To demonstrate our new implementation, we compare the performance of sequential assimilation and all-at-once assimilation on a synthetic problem and on a real-world paleoclimatic reconstruction application (20th century reanalysis). The climate reconstructions provided by the different assimilation techniques are compared using scoring rules [17], which, though not broadly used in climatology, allow for a finer assessment of reconstruction quality by considering the full probabilistic nature of the assimilation compared to more traditional metrics that only treat the reconstruction as a pointwise prediction.

This paper is structured as follows: in Section 2 we review the basics of the ensemble Kalman filter and its variants. In Section 3 we introduce the distributed ensemble Kalman filter (dEnKF) and demonstrate its capabilities.

Finally, in Section 4, we compare the performances of all-at-once assimilation with sequential assimilation in synthetic experiments as well as on real-world large-scale climate reconstruction problems.

Our study shows that all-at-once assimilation performs significantly better on all considered problems, while still being computationally tractable. This opens new venues for the study of the effects of covariance localization in climate reconstruction [43] and provides the first large-scale extension of the investigations on sequential vs synchronous assimilation performed in [34] that were limited to small-scale setups, due to lack of computational resources.

2 The Kalman Filter and its Variants

Ensemble Kalman filtering (EnKF) is a data assimilation technique that aims at providing an estimation of the state of a dynamical system by combining observed data with a prior model of the unknown system state. Before going into the details of the EnKF, we review the classic (discrete) Kalman filter, adopting a Bayesian point of view for our exposition. The interested reader is referred to [40] and [45] for more details. The exposition presented here is inspired from the one in [28].

In the following, let $\psi_t^* \in \mathbb{R}^m$ denote the unknown state vector of some physical system at time t and assume that the system is governed by the following dynamics

$$\psi_{t+1}^* = \mathcal{F}_t \psi_t^* + \delta_t, \quad \delta_t \sim \mathcal{N}(0, \mathbf{\Delta}_t), \quad (1)$$

where, for all $t \in \mathbb{N}$, the dynamics of the system is determined by a linear operator $\mathcal{F}_t : \mathbb{R}^m \rightarrow \mathbb{R}^m$ and δ_t is a random vector modelling our uncertainty in the dynamics of the system. In what follows, we always assume that δ_t is independent of $\delta_{t'}$ for $t \neq t'$.

At each time step t , we are given observations that stem from a linear operator \mathbf{G}_t applied to the current unknown state of the system:

$$\mathbf{y}_t = \mathbf{G}_t \psi_t^* + \epsilon_t, \quad \epsilon_t \sim \mathcal{N}(0, \mathbf{E}_t), \quad (2)$$

where $\mathbf{G}_t : \mathbb{R}^m \rightarrow \mathbb{R}^{n_t}$ is a linear measurement operator and ϵ_t is a random observation noise vector. We assume that ϵ_t is independent of $\epsilon_{t'}$ for $t \neq t'$. Kalman filtering aims at sequentially estimating (filtering) the state of the system, based on the observations available up to the current time step and on some prior knowledge about the initial state at time 0. In a Bayesian formulation, Kalman filtering assumes that the initial state ψ_0 is a realization of random vector Ψ_0 with Gaussian prior distribution $\Psi_0 \sim \mathcal{N}(\boldsymbol{\mu}_0, \boldsymbol{\Sigma}_0)$ and then approximates the unknown state at time t using the posterior (filtering) distribution of Ψ_0 conditionally on the dynamics and the observations up to t . This conditional distribution is Gaussian with mean and covariance that are given by:

$$\boldsymbol{\mu}_t = \boldsymbol{\mu}_t^f + \mathbf{K}_t \left(\mathbf{y}_t - \mathbf{G}_t \boldsymbol{\mu}_t^f \right), \quad (3)$$

$$\boldsymbol{\Sigma}_t = \boldsymbol{\Sigma}_t^f - \mathbf{K}_t \mathbf{G}_t \boldsymbol{\Sigma}_t^f, \quad (4)$$

where the matrix \mathbf{K}_t is called the *Kalman gain* and is given by

$$\mathbf{K}_t = \boldsymbol{\Sigma}_t^f \mathbf{G}_t^T \left(\mathbf{G}_t \boldsymbol{\Sigma}_t^f \mathbf{G}_t^T + \mathbf{E}_t \right)^{-1}, \quad (5)$$

assuming the matrix in parenthesis to be invertible, and the *forecast mean* $\boldsymbol{\mu}_t^f$ and *forecast covariance* $\boldsymbol{\Sigma}_t^f$ are given by:

$$\begin{aligned} \boldsymbol{\mu}_t^f &= \mathcal{F}_t \boldsymbol{\mu}_{t-1}, \\ \boldsymbol{\Sigma}_t^f &= \mathcal{F}_t \boldsymbol{\Sigma}_{t-1} \mathcal{F}_t^T + \mathbf{\Delta}_t. \end{aligned}$$

The key quantity to compute at each iteration is the *Kalman gain*, which is a $m \times n_t$ matrix. In practice, the use of the above Kalman filter algorithm requires computing the $m \times m$ conditional covariance matrix $\boldsymbol{\Sigma}_t$ at each step, which can be prohibitive or even impossible when the state space is large, as in the case, for example, in climate science applications. The Ensemble Kalman Filter (EnKF) was introduced to overcome these difficulties.

2.1 Ensemble Kalman Filter

The ensemble Kalman filter (EnKF) can be seen as a Monte-Carlo approximation of the classical Kalman filter that aims at bypassing the difficulties created by large conditional covariance matrices. Its key idea is to approximate the conditional distribution at each step by a sample (ensemble) drawn from the distribution. Then,

instead of having to update mean vectors and covariance matrices, one only has to update the ensemble members, thereby reducing the computational burden and memory footprint.

Considering the same setting as in the previous section, ensemble Kalman filtering begins with an *ensemble*, $\psi_0^{(1)}, \dots, \psi_0^{(p)} \stackrel{\text{i.i.d.}}{\sim} \mathcal{N}(\mu_0, \Sigma_0)$ which is a sample from the prior state distribution. At each step $t \in \mathbb{N}$, the EnKF updates the current ensemble members $\psi_{t-1}^{(1)}, \dots, \psi_{t-1}^{(p)}$ to a new ensemble $\psi_t^{(1)}, \dots, \psi_t^{(p)}$ so that the new ensemble constitutes an i.i.d. sample of the conditional distribution at time t . The traditional EnKF produces an ensemble that approximates the conditional distribution by updating the mean and deviations using *perturbed observations*. Indeed, as noted by [5], one needs to inject randomness at each update step so that the filter does not underestimate the variance. The complete EnKF update procedure is described in Algorithm 1. We note that the Gaussianity assumption on the ensemble can be dropped and refer the reader to [19] for a review of some non-Gaussian extensions of the EnKF.

Algorithm 1 EnKF update (perturbed observations)

Require: Ensemble $\psi_{t-1}^{(1)}, \dots, \psi_{t-1}^{(p)}$, observation operator G_t , observed data \mathbf{y}_t and observation noise covariance matrix E_t .

Ensure: Updated ensemble $\psi_t^{(1)}, \dots, \psi_t^{(p)}$.

1. Sample evolution errors $\delta_t^{(i)} \stackrel{\text{i.i.d.}}{\sim} \mathcal{N}(0, \Delta_t)$.
2. Forecast members

$$\psi_t^{f(i)} = G_t \psi_{t-1}^{(i)} + \delta_t^{(i)}.$$

3. Sample *perturbed observations* $\mathbf{y}_t^{(i)} \stackrel{\text{i.i.d.}}{\sim} \mathbf{y}_t + \epsilon_t$
4. Estimate *ensemble covariance matrix* $\hat{\Sigma}_t$ and compute *Kalman gain*:

$$\hat{K}_t = \hat{\Sigma}_t G_t^T (G_t \hat{\Sigma}_t G_t^T + E_t)^{-1}$$

5. Update the ensemble members:

$$\psi_t^{(i)} = \psi_t^{f(i)} + \hat{K}_t (\mathbf{y}_t^{(i)} - G_t \psi_t^{f(i)}). \quad (6)$$

Here, compared to the traditional Kalman filter, one does not have access to the forecast covariance matrix Σ_t^f , so that one has to replace it by some estimator $\hat{\Sigma}_t^f$ computed from the ensemble. There exists various techniques for estimation of the forecast covariance, such as localization [24, 22], shrinkage [29, 30], Bayesian estimation [9, 20], some of which are further explained in Section 2.3.

One sees that, at each step, the EnKF maintains an ensemble of p state vectors that approximates the conditional distribution, and that the update equations are analogous to the classical Kalman update equations, with the state forecast covariance replaced by some ensemble estimate thereof and the observations replaced by perturbed ones. The ensemble update equations Equation (6) were chosen so that, in the limit of infinite ensemble size, the empirical ensemble covariance converges to the true covariance. Although theoretically justified, the use of perturbed observations at every step is a source of sampling errors that reduces filter performances at small ensemble sizes (see [47] for a detailed study). Therefore, deterministic approaches that avoid the use of perturbed observations have been developed. Most of these approaches fall under the category of *square root filters* [41], which we present next.

2.2 Ensemble Square Root Filters

Ensemble square root filters (EnSRF) are a class of ensemble Kalman filters that use deterministic updates to avoid the use of perturbed observations [47, 41]. As for the EnKF, our exposition of EnSRF will mostly follow the one in [28] and we refer interested readers to this work for more details and to [25] for a review of the different types of ensemble Kalman filters.

Denoting by $\bar{\psi}_t$ the mean of the ensemble members at time t and by $\psi_t^{(i)'} := \psi_t^{(i)} - \bar{\psi}_t$ the deviations of the ensemble members from the mean, the EnSRF replaces the update equations of the EnKF by an update of the

mean and an update of the deviations:

$$\bar{\psi}_t = \bar{\psi}_t^f + \hat{K} \left(\mathbf{y}_t - \mathbf{G} \bar{\psi}_t^f \right), \quad (7)$$

$$\psi_t^{(i)'} = \psi_t^{f(i)'} - \tilde{K}_t \mathbf{G} \psi_t^{f(i)'}, \quad (8)$$

where the *square root Kalman gain* \tilde{K}_t is a matrix defined by:

$$\tilde{K}_t = \hat{\Sigma}_t^f \mathbf{G}_t^T \left(\sqrt{\mathbf{G}_t \hat{\Sigma}_t^f \mathbf{G}_t^T + \mathbf{E}_t} \right)^{-1} \left(\sqrt{\mathbf{G}_t \hat{\Sigma}_t^f \mathbf{G}_t^T + \mathbf{E}_t} + \sqrt{\mathbf{E}_t} \right)^{-1}, \quad (9)$$

and the mean and deviations are updated deterministically: $\bar{\psi}_t = \mathbf{G}_t \bar{\psi}_t$, $\psi_t^{f(i)'} = \mathbf{G}_t \psi_{t-1}^{f(i)'}$. In the above, we assume the matrices in parenthesis to be invertible, and the square roots are allowed to be any matrix square root of the original matrix. The EnSRF has been found to overperform the EnKF with perturbed observations for small ensemble sizes [47].

2.3 Sequential Filtering and the Problem of Localization

When using ensemble Kalman filters, great care has to be taken in the choice of the ensemble forecast covariance estimator $\hat{\Sigma}_t^f$ that is used for the definition of both the *ensemble Kalman gain* in the EnKF Equation (6) and of the *square root Kalman gain* in the EnSRF Equation (9). Indeed, in most applications, the ensemble size is drastically smaller than the state vector, so that estimators based on the empirical covariance of the ensemble will suffer from errors due to undersampling. Furthermore, the empirical covariance may fail to be positive-definite and thus fail to be invertible. The issues call for sophisticated estimation procedures for the forecast covariance matrix.

For spatial data assimilation problems, the undersampling errors are typically known to manifest themselves as so-called spurious correlations between distant locations. *Localization* is a procedure to mitigate those and produce a better estimate of the ensemble covariance than the empirical one [24, 22]. The idea behind localization is to taper the long-range correlations in the empirical covariance by using a distance-dependent smoothing. Formally, *localization* estimates the ensemble forecast covariance matrix by

$$\hat{\Sigma}_t^f = \text{Cov} \left(\left(\psi_t^{f(i)} \right)_{i=1, \dots, p} \right) \circ \rho,$$

where the first term denotes the empirical covariance of the ensemble forecast, ρ is a prescribed symmetric positive-definite *localization matrix* and \circ denotes elementwise product. The *localization matrix* ρ is usually chosen according to the characteristics of the problem at hand. In applications where the state vector represents the values of some spatially varying field $f : \mathbb{R}^d \times \mathbb{R} \rightarrow \mathbb{R}$, $(\psi_t)_j = f(x_j, t)$, localization matrices are typically defined by applying a symmetric positive definite function ρ to the spatial locations so that $\rho_{jk} = \rho(x_j, x_k)$. We note that there also exists non-distance-based localization approaches, such as the ones developed by [15].

2.3.1 Sequential Filtering

Even though the EnKF algorithm alleviates some of the computational burdens of the traditional Kalman filter by bypassing the update of the forecast covariance matrix, the implementation of the update equations Equations (7) and (8) is still fraught with potential memory overflows resulting from the computation of the square root Kalman gain matrix \tilde{K}_t . Indeed, for a state space of dimension m , the computation of the Kalman gain still requires building the $m \times m$ estimated covariance matrix $\hat{\Sigma}_t$, so that one quickly runs into bottlenecks for state spaces of moderate dimensions. One way to circumvent this is to assimilate the available observations sequentially, one at a time [24].

In this variant of the EnKF, at any given assimilation step t , given a data vector \mathbf{y}_t of size n_t and an observation operator \mathbf{G}_t , one assimilates the individual data points $\mathbf{y}_{t,j}$ sequentially by using the update equations Equations (7) and (8) for each observation and then using the updated ensemble as a starting point for the assimilation of the next observation. Note that such an assimilation scheme is only valid as long as the observations errors are uncorrelated. When assimilating only observation number i , the critical quantity to be computed is the product $\hat{\Sigma}_t (\mathbf{G}_t^T)_{:j}$, where $(\mathbf{G}_t^T)_{:j}$ denotes the j -th column of \mathbf{G}_t . Being of the same dimension m as the state space, this product can easily be stored once computed and no further memory bottlenecks arise down the assimilation pipeline; nevertheless, the computation of the product still requires some care to handle the large matrix $\hat{\Sigma}_t$. While there exists approaches that deal with more general observations, such as linear forms [42], we here focus on the case where only pointwise observations of the state are available, i.e. $(\mathbf{G}_t)_{j,:}$ is 1 at index ℓ_j and 0 elsewhere. In such settings, the product then involves only a single column of the estimated covariance matrix,

drastically simplifying the computations. Algorithm 2 gives a detailed account of the assimilation procedure, assuming that at step t the available data is made of observations of the state vector at indices $\ell_1, \dots, \ell_{n_t}$, that is, the forward operator can be written as $(\mathbf{G}_t)_{jk} = \delta_{k\ell_j}$ (note that for completeness we should add a time index to the ℓ_j 's, but we drop it for the sake of readability).

Algorithm 2 EnSRF update (sequential version)

Require: Ensemble $\psi_{t-1}^{(1)}, \dots, \psi_{t-1}^{(p)}$, observation operator \mathbf{G}_t , observed data \mathbf{y}_t and observation noise covariance matrix \mathbf{E}_t .

Ensure: Updated ensemble $\psi_t^{(1)}, \dots, \psi_t^{(p)}$.

1. Forecast members (deterministically)

$$\psi_t^{f(i)} = \mathcal{F}_t \psi_{t-1}^{(i)}.$$

2. **for** each observation $\mathbf{y}_{t,j}$ and corresponding observation index ℓ_j **do**:

- 2.1. Estimate corresponding column $(\hat{S}t)_{:j}$ of the sample covariance.
- 2.2. Apply localization $(\hat{\Sigma}t)_{:j} = \boldsymbol{\rho} \circ (\hat{S}t)_{:j}$.
- 2.3. Compute the single observation Kalman gains

$$\begin{aligned} \mathbf{K}_t &= (\hat{\Sigma}t)_{:j} \left((\hat{\Sigma}t)_{jj} + \mathbf{E}_t \right)^{-1} \\ \tilde{\mathbf{K}}_t &= (\hat{\Sigma}t^f)_{:j} \left(\sqrt{(\hat{\Sigma}t^f)_{jj} + (\mathbf{E}t)_{jj}} \right)^{-1} \left(\sqrt{(\hat{\Sigma}t^f)_{jj} + (\mathbf{E}t)_{jj}} + \sqrt{(\mathbf{E}t)_{jj}} \right)^{-1}, \end{aligned}$$

and update the ensemble members to get $\psi_t^{(i)}$.

- 2.4. Use update as background for next assimilation:

$$\psi_t^{f(i)} \leftarrow \psi_t^{(i)}. \tag{10}$$

In the sequential EnSRF Algorithm 2, localization is applied at every assimilation step. It turns out that this interplay of localization and sequential assimilation makes the update equations inconsistent, as was already noted by [47]. Indeed, in order to correctly implement sequential, localized ensemble square root Kalman filtering, one would need to first localize the whole sample covariance matrix and update the full matrix at every step, resulting in no computational savings compared to non-sequential assimilation.

While it is well known in the data assimilation community that the interplay of localization and sequential assimilation produces inconsistent results, little effort has been devoted to studying the magnitude of these inconsistencies and to fixing them. To the best of our knowledge, the only systematic study of this phenomenon has been undertaken by [34], which identified that, in such cases, assimilation results depend on observation ordering and that inconsistencies can become significant when observational errors are similar in magnitude to model errors. Our goal in the rest of this work is to provide a distributed implementation of the EnSRF (Section 3) that allows for the assimilation of large datasets in a non-sequential fashion. By leveraging distributed computing, our *all-at-once* (aao) assimilation algorithm is able to bypass the need for sequential processing and thus uses a consistent update scheme. Then, in Section 4 we provide detailed comparisons of the performance of our all-at-once assimilation algorithm compared to sequential assimilation on both toy examples and real test cases.

3 Distributed Non-Sequential Ensemble Kalman Filtering

In order to overcome the memory bottlenecks that plague the ensemble Kalman filter, we turn to distributed computing techniques, with the goal of storing the full estimated state covariance matrix (which represents the main roadblock) in distributed memory. For our implementation, we use the DASK [37, 8] Python library, which is a framework that allows for seamless handling of distributed arrays and provides a chunked implementation of most traditional array algorithms.

In DASK, large arrays are chunked and stored split across several nodes in a computing cluster, while still providing a programming interface that allows for writing algorithms as if one were operating with a regular array. In a Kalman filtering context, this means that one is no longer limited by the storage of the state covariance

matrix, as long as it can fit on the available computing cluster. We note that apart from storing the covariance matrix, there are two other operations in the EnSRF algorithm that are problematic when this matrix is large: computing its inverse and square root. Thankfully, inverses and square roots can be (approximately) computed in distributed memory by using the randomized SVD algorithm from [21], which is implemented in DASK as `dask.array.linalg.compressed_svd`.

We stress that the idea of using randomized SVD in ensemble Kalman filter has already been developed elsewhere, most notably in [4, 13]. While our work shares this central idea with the ones just cited, our originality is threefold: i) we provide a **distributed** implementation in a user-friendly Python package, ii) we perform a **detailed study of the improvements** of all-at-once assimilation over the sequential one and iii) we demonstrate our algorithm on **large-scale** problems. On the other hand, the previously cited works do not provide a distributed implementation and do not compare themselves to sequential assimilation.

We now turn to the practical implementation of the EnSSRF algorithm in a distributed computing framework. In the following, let λ_i and $u_i, i = 1, \dots, k$ be the k -largest (approximate) singular values and corresponding left singular vectors of the estimated background covariance $\hat{\Sigma}$ delivered by the rank k randomized truncated SVD algorithm of [21]. Then, one can compute approximate inverses and square roots of $\hat{\Sigma}$ via:

$$\hat{\Sigma}^{-1} \approx [u_1, \dots, u_k] \begin{pmatrix} 1/\lambda_1 & & \\ & \ddots & \\ & & 1/\lambda_k \end{pmatrix} [u_1, \dots, u_k]^T$$

$$\sqrt{\hat{\Sigma}} \approx [u_1, \dots, u_k] \begin{pmatrix} \sqrt{\lambda_1} & & \\ & \ddots & \\ & & \sqrt{\lambda_k} \end{pmatrix} [u_1, \dots, u_k]^T.$$

Thanks to these approximations, one only has to store k singular values and m -dimensional singular vectors, providing substantial computational savings compared to the m^2 needed for the full covariance matrix. We note furthermore that since the DASK library is based on lazy evaluation, the approximate inverse and square roots are never fully computed, only the relevant parts are built at runtime. Based on the above, let us define the procedures `APPROXIMATEINVERSE` $((\lambda_i, u_i)_{i=1, \dots, k})$ and `APPROXIMATESQRT` $((\lambda_i, u_i)_{i=1, \dots, k})$, which, given the first k approximate singular values and left singular vector λ_i and $u_i, i = 1, \dots, k$ of a matrix compute the approximate inverse, respectively the approximate square root of the matrix. On top of these, let us also define the procedure

`KALMANUPDATE` $((\psi_t^{(i)})_{i=1, \dots, p}, \mathbf{G}_t, \mathbf{y}_t, \hat{\Sigma}_t^{-1}, \sqrt{\hat{\Sigma}_t})$, which performs the (ensemble square root) Kalman update eqs. (7) and (8) for a given ensemble and observations, given precomputed inverses and square roots of the estimated state covariance matrix. Using these, we can now formulate an algorithm for a distributed implementation of a single step of the Ensemble Square Root Kalman Filter:

Algorithm 3 Distributed EnSRF update

Require: Ensemble $\psi_{t-1}^{(1)}, \dots, \psi_{t-1}^{(p)}$, observation operator \mathbf{G}_t and observed data \mathbf{y}_t
SVD cutoff rank k .

Ensure: Updated ensemble $\psi_t^{(1)}, \dots, \psi_t^{(p)}$.

Build localized estimated covariance $\hat{\Sigma}_t$ in distributed memory.

$(\lambda_i, u_i)_{i=1, \dots, k} \leftarrow \text{DISTRIBUTEDSVD}(\hat{\Sigma}_t, \text{rank} = k)$

$\hat{\Sigma}_t^{-1} \leftarrow \text{APPROXIMATEINVERSE}((\lambda_i, u_i)_{i=1, \dots, k})$

$\sqrt{\hat{\Sigma}_t} \leftarrow \text{APPROXIMATESQRT}((\lambda_i, u_i)_{i=1, \dots, k})$

$(\psi_t^{(i)})_{i=1, \dots, p} \leftarrow \text{KALMANUPDATE}((\psi_t^{(i)})_{i=1, \dots, p}, \mathbf{G}_t, \mathbf{y}_t, \hat{\Sigma}_t^{-1}, \sqrt{\hat{\Sigma}_t}) \quad \triangleright$ Update using eqs. (7) and (8)

When implemented in a lazy-evaluation framework such as DASK, the memory requirements of Algorithm 3 are twofold: first there should be enough memory to build the estimated state covariance matrix (localized) $\hat{\Sigma}_t$ second there should be enough memory left to compute the approximate SVD of this matrix. Once this is done, memory can be cleared and only the first k singular values and left singular vectors need to be stored. In the

following section, we demonstrate how our distributed implementation of the EnSRF algorithm allows for non-sequential (all-at-once) assimilation in large-scale problems and show how it outperforms sequential assimilation (which uses inconsistent update equations, see Section 2.3.1) on both a synthetic test case and a paleoclimatic reconstruction problem.

4 Experimental Comparison of Sequential and Non-Sequential Filtering

Even if non-sequential ensemble Kalman filtering is theoretically guaranteed to overperform its sequential counterpart when the assumptions of the Kalman filter are met; practical applications of the EnKF almost always lie outside of the validity range of these assumptions. We thus here provide numerical comparisons between all-at-once (aao) and sequential (seq) assimilation schemes for the EnKF on practical assimilation problems. In order to compare performances, we run the two schemes in a variety of different scenarios where ground-truth for the state to be estimated is available. We assess the reconstruction quality of the approaches using three different metrics:

- Root mean-square error (RMSE) when predicting with the analysis mean,
- RMSE skill score [7],
- Energy score (ES) multivariate scoring rule [18].

While the first two are commonly used metrics in the Kalman filter community, scoring rules have yet to see broad application in those fields. Compared to the other metrics, the energy score takes the full analysis ensemble into account and also allows for theoretically sound ranking of different models. These scoring rules are explained in more details in the coming sections.

4.1 Synthetic Test Case

We first compare the all-at-once (aao) and sequential (seq) implementation of the EnKF on a synthetic test case. The task is to reconstruct a two-dimensional scalar field on the unit square, discretized on a $m \times m$ square grid. The ground truth is generated by sampling a Matérn 3/2 Gaussian process (GP) with unit variance and correlation length $\lambda = 0.1$. A starting ensemble (background) is also generated by sampling p realizations from the same process, putting ourselves in a "well-specified" setup. All-at-once and sequential implementations are then compared by assimilating n data points at randomly chosen locations.

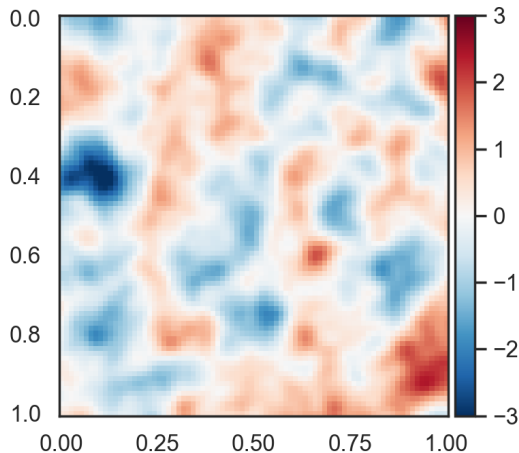


Figure 1: Example of ground truth sampled from the GP model.

To compare the two assimilation schemes, a set of 20 different ground truths is generated by sampling from the aforementioned GP model. For each such realization, a starting ensemble of size 30 is also sampled from the same GP model, the number of ensemble members being chosen such as to reproduce situations encountered in practice. Then, a set of $n = 1000$ randomly chosen data points is assimilated using each scheme and the assimilation results are compared using the aforementioned metrics. The ground truth are discretized on a 80×80 square grid and the goal is to reconstruct the discretized ground truth vector. Figure 1 and fig. 2 depict the starting setup for one iteration of the experiments. The observational noise standard deviation is set to $\sigma_\epsilon = 0.01$, which corresponds to 1% of the standard deviation of the GP model used to generate the ground truths and

the ensembles. The effect of the observational noise level on the assimilation is further studied in follow-up experiments.

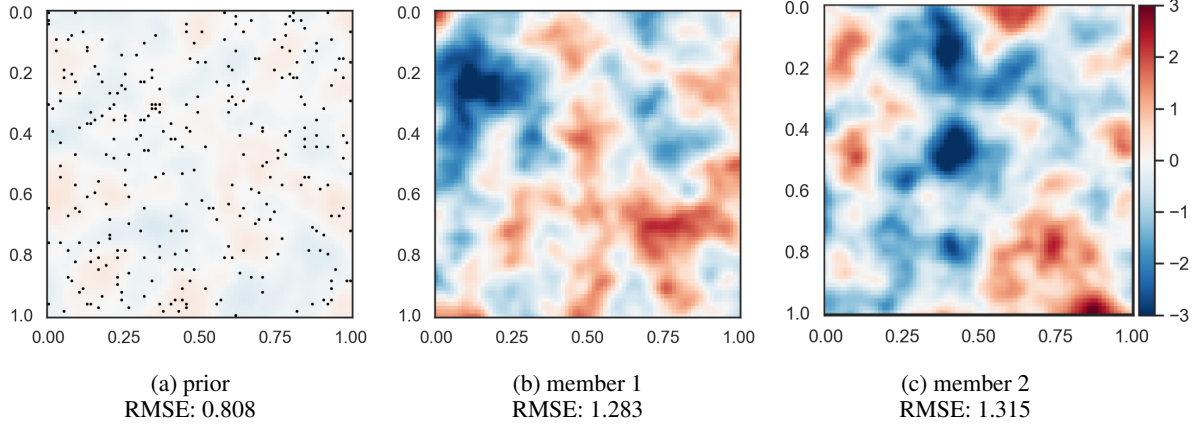


Figure 2: Prior mean (a) and selected prior ensemble members (b) and (c). Observation locations depicted in black. RMSE for prediction of the ground truth in fig. 1 also depicted for each member.

The covariance localization used in the experiment was composition with a symmetric positive definite function (see section 2.3). The localization function used was a Matérn 3/2 kernel [35] with correlation length set to 0.2 (twice the one of the GP used to generate the ground truths). We note that this choice is arbitrary but was made to strike a compromise between realism (one does not know the “right” localization function in practice) and reconstruction quality.

Results for assimilation of the data corresponding to the ground truth from Figure 1 are depicted in Figure 3. No obvious qualitative differences between the two assimilation schemes are to be found. Quantitative differences can be computed by considering, the root-mean-square error (RMSE) when reconstructing the ground truth using the data assimilation results. The RMSE when predicting the ground truth with the updated mean and two selected ensemble members is also depicted in Figure 3 for each assimilation scheme. One sees that all-at-once assimilation tends to perform better than the sequential approach.

In order to get a quantitative assesment of the difference in accuracy between sequential and all-at-once assimilation, we repeat the assimilation experiments 20 times by sampling different ground truth from the GP model described before. Apart from the reconstruction RMSE, one can also compute the difference in the *RMSE skill score* for the different schemes. The *RMSE skill score* [33] is a widely used metric for ranking model performances in atmospheric science. For a given set of forecast vectors ψ_t^f , the RMSE skill score aims at assessing how well the forecast improves the reconstruction a given reference ψ_t^r compared to some original background forecast ψ_t^b , over some time period $t \in T$. The RMSE skill score is given by (time index ommited for brevity):

$$\text{RMSE}_{\text{ess}}(\psi^f, \psi^r, \psi^b) := 1 - \frac{\sum_{t \in T} \|\psi_t^f - \psi_t^r\|^2}{\sum_{t \in T} \|\psi_t^b - \psi_t^r\|^2}$$

Note that while the original definition of the RMSE skill score does not include a time dimension, it is customary in climate science to sum over the considered time steps. Compared to the RMSE, this metric weighs the errors by the best improvement that can be achieved, i.e. errors where the background is far from the reference are penalized less heavily. The RMSE skill score ranges from 1 to $-\infty$, with a value of 1 corresponding to perfect reconstruction. Figure 4 shows the distribution of the RMSE and RMSE skill score for sequential and all-at-once assimilation. Since these results depend on the choice of localization used, we also include the results for all-at-once assimilation using the true covariance matrix that was used to generate the ground truth. This gives an idea of the best possible reconstruction that can be achieved under the current conditions.

We see that all-at-once outperforms sequential assimilation for all metrics by an order of 2 to 5% (see [46] on interpreting skill scores).

While the RMSE skill score is widely used in climate science, it has been pointed out in the literature [46] that skill scores can be misleading and biased compared to raw scores. Also, we would like to stress that, in the context of ensemble Kalman filters, the RMSE skill score does not leverage the full content of the forecast

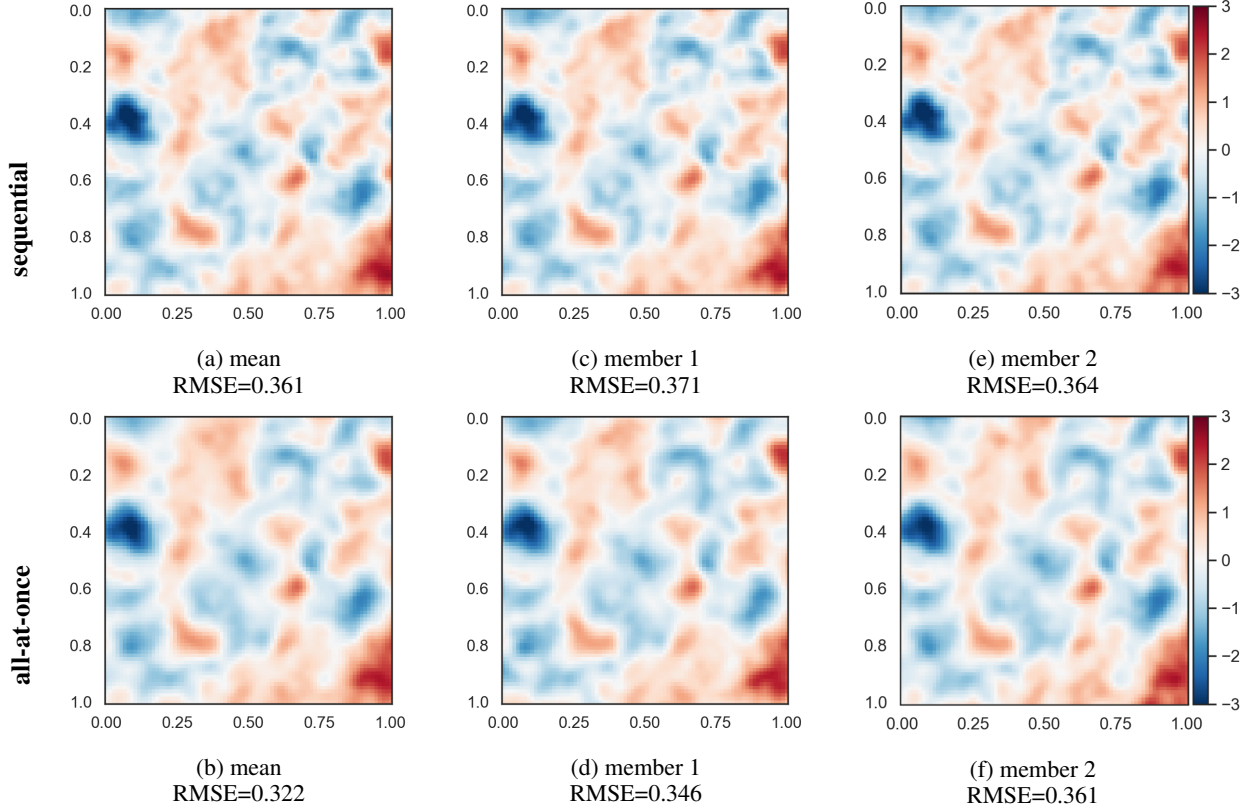


Figure 3: Updated means and selected updated ensemble members, after assimilation of the data generated from the ground truth in Figure 1.

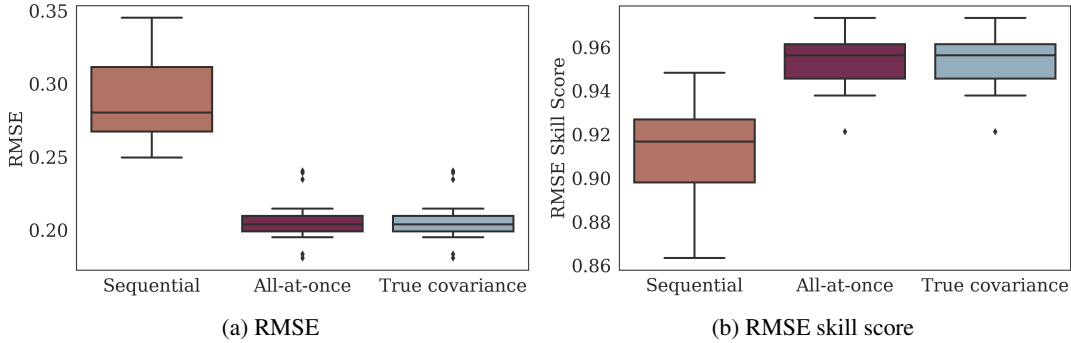


Figure 4: Comparison of the distributions (20 repetitions) of the RMSE and RMSE skill score (**synthetic test case**).

since it only considers pointwise prediction (ensemble mean) when we have a full ensemble at hand. In order to incorporate the probabilistic information contained in the spread of the forecast ensemble in the ranking of the assimilation schemes, one should use *proper scoring rules* [17]. We here only focus on the *energy score* (ES) [18], which is a proper scoring rule for multivariate forecasts. For a given ensemble of forecast vectors $\psi_t^f, i = 1, \dots, p$ and a reference vector ψ_t^r to be reconstructed, the energy score is given by [26]:

$$\text{ES}(\psi_t^{f^{(i)}}, \psi_t^r) := \frac{1}{p} \sum_{i=1}^p \|\psi_t^{f^{(i)}} - \psi_t^r\| - \frac{1}{2p^2} \sum_{i=1}^p \sum_{j=1}^p \|\psi_t^{f^{(i)}} - \psi_t^{f^{(j)}}\|$$

Scoring rules are used for model comparison and ranking, lower scores corresponding to better models, according to the scoring at hand. While the energy score has some shortcomings (see [3] for a review and presentation

of alternative scoring rules), such multivariate scoring rules have yet to find broad use in climate science and we firmly believe that the multivariate and probabilistic nature of ES already offers an improvement over the univariate point-prediction scorings used in the community. Figure 5 shows that all-at-once also outperforms sequential assimilation in terms of energy score.

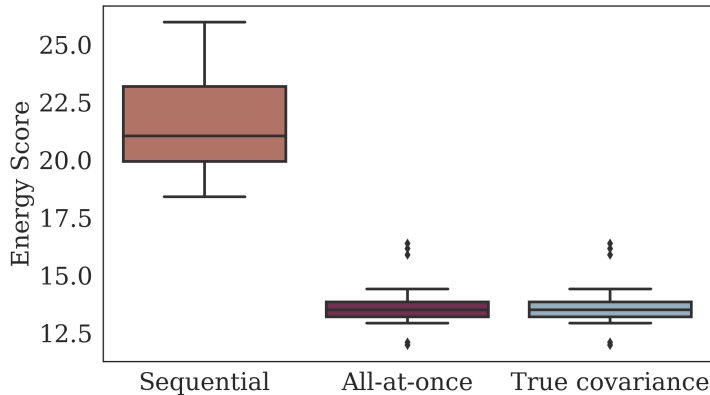


Figure 5: Comparison of the energy score for the different assimilation methods (**synthetic test case**).

The amount by which all-at-once and sequential assimilation differ for the EnSRF depends on the magnitude of the observation errors compared to the spread of the starting ensemble. Indeed, as noted by [34] “*When the observation errors [are] of a similar magnitude as the initial errors of the state estimate, both filter methods [show] a similar behavior. When the observation errors [are] decreased, the EnSRF [shows] a stronger tendency to diverge and larger minimum RMS errors [...] than variant of the EnSRF that assimilates all observations at once.*” Figure 6 demonstrates this effect by increasing the observational error standard deviation σ_ϵ . Degradation of performance for the sequential EnSRF at small observational errors is clearly visible.

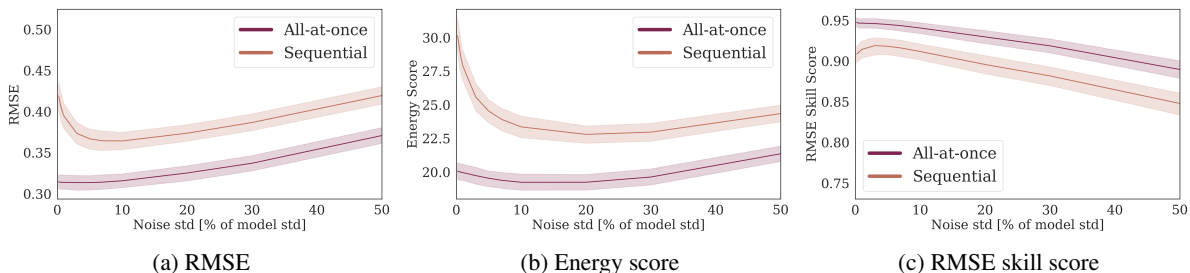


Figure 6: Evolution of the different accuracy metrics as a function of the observational noise standard deviation (**synthetic test case**).

On top of the above effect, incorrect updates in the localized, sequential version of the EnSRF introduce dependencies on the order of the observations, as was also noted by [34]. While this effect is well known in the data assimilation community, it is usually assumed to be of little practical relevance. Apart from the small-scale experiments (40 observations) performed by [34], evidence for this assumption is lacking. To study the effect of ordering in larger assimilation setups, we use the same setting as above (80×80 grid, $p = 30$ ensemble members, $n = 300$ observations) and randomly permute the order of the observations before assimilation. Figure 7 compares the performance of sequential and non-sequential assimilation for 50 different random orderings of the same dataset.

The experiments demonstrate that in a sequential setting, observation ordering can have an effect of roughly 5% on the assimilation performance, thus confirming the results of [34] and providing further proof that sequential assimilation is not consistent. As expected, all-at-once assimilation shows no dependence on data ordering.

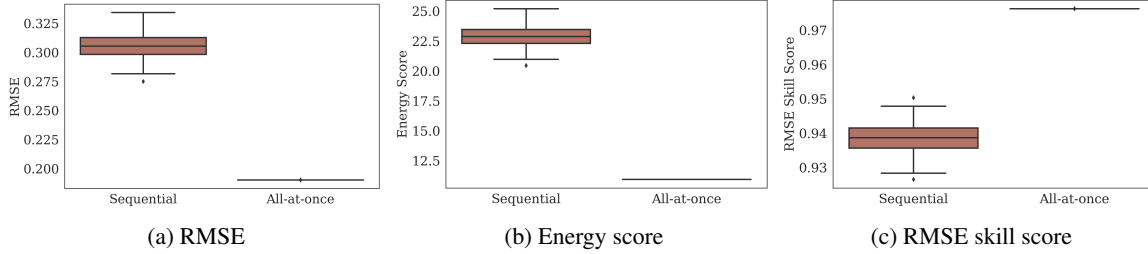


Figure 7: Comparison of the distributions of the accuracy metrics for different observation orderings using sequential assimilation (**synthetic test case**).

4.1.1 Computational Capabilities and Limitations

Even if all-at-once assimilation outperforms sequential assimilation in terms of reconstruction performance, as was shown in the previous section, there is still a computational overload associated to the computation of the full state covariance matrix. This results in a memory footprint that grows quadratically with the state dimension. In order to get a rough understanding of the limitations of all-at-once assimilation, it is worth studying the dependence of the memory footprint and total runtime on the dimension of the state vector.

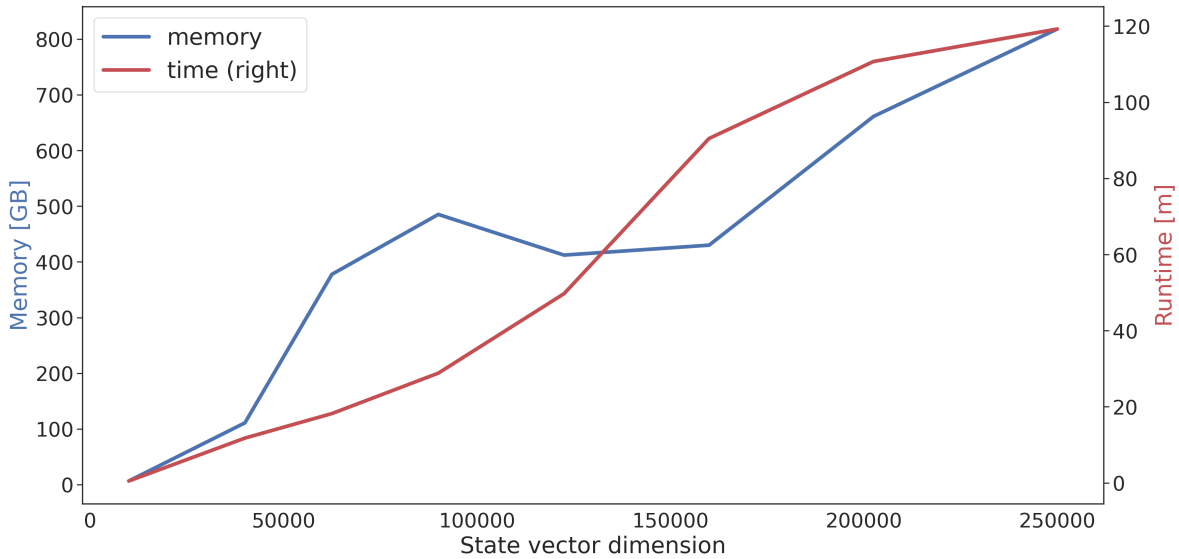


Figure 8: Peak memory usage and total runtime for all-at-once assimilation of 10000 data points as a function of the state dimension.

Figure 8 depicts the peak memory use and total runtime for assimilation of 10000 data points using our implementation of all at once assimilation for the EnSRF (see Section 3). The assimilation is run on a multi-node computing cluster managed by SLURM [49] and the number of nodes dedicated to the assimilation is allowed to grow if available memory becomes tight. For this reason, total memory usage and runtime depicted in Figure 8 should be considered more as rough estimates that showcase the capabilities of our implementation, since in practice, the total memory use will fluctuate depending on the hardware and specific settings of the cluster. The above results demonstrate that our framework is able to perform covariance localization and ensemble Kalman filtering in state spaces of dimension up to 250000, which, in climate reconstruction applications, would correspond to performing reconstruction of several correlated climate variables on a high-resolution grid. Overall, those results indicate that our all-at-once assimilation framework is able to scale to realistic application settings, thus paving the way for the use of non-sequential assimilation in paleoclimate reconstruction tasks and other large-scale data assimilation problems.

4.2 Paleoclimate Reconstruction Test Case

In order to demonstrate the superiority of all-at-once EnSRF assimilation over the sequential one on real-world problems, we now turn to a paleoclimate reconstruction task and perform the same comparisons as in the last section. This application reproduces a popular Kalman-based method for climate and weather reconstruction [2, 6, 39, 14]. The idea is to blend historical observations with climate models simulations to get a global reconstruction of past climate states.

The goal of our paleoclimatic reconstruction task is to reconstruct monthly average temperatures for the period 1960-1980 using an EnSRF. As a reference (ground truth) for the climate state over this period, we use the *Climatic Research Unit gridded Time Series* (CRU TS) dataset [23]. CRU TS is a high-resolution (0.5° by 0.5°) dataset of monthly reconstructed climate variables (mean temperature, precipitation rate, ...) produced by interpolating station data. For our practical purpose, this dataset can be considered as embodying the state of the art in climate reconstruction. Our starting ensemble is a set of 30 model simulations from the general circulation model *ECHAM5.4* [38] discretized on a 192 grid and is the same as used for several state-of-the-art climate reconstructions [2, 14]. The simulations incorporate known external forcings such as solar irradiance, volcanic activity and greenhouse gas concentration. To bring the simulations back towards reality, we assimilate station data of monthly average temperature. The dataset used for the station data is the *international surface temperature initiative (ISTI) global land surface databank stage 3 station dataset* [36]. Figure 9 shows an overview of the stations available in the dataset for January 1960.

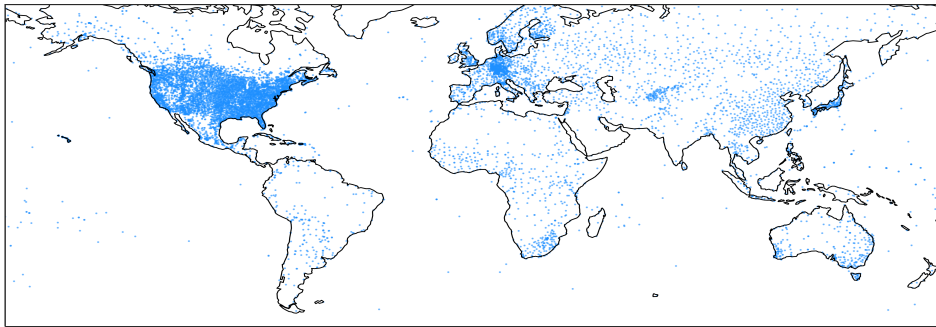


Figure 9: Stations in the ISTI dataset for January 1960.

As for the synthetic test case, we compare the RMSE skill score, energy score and RMSE for the different assimilation schemes. Figures 10 and 11 show the monthly RMSE and ES and demonstrates how all-at-once assimilation outperforms sequential assimilation by a magnitude that is often of half a degree in the RMSE. Similarly, the energy score also indicates that all-at-once assimilation should be preferred over the sequential one.

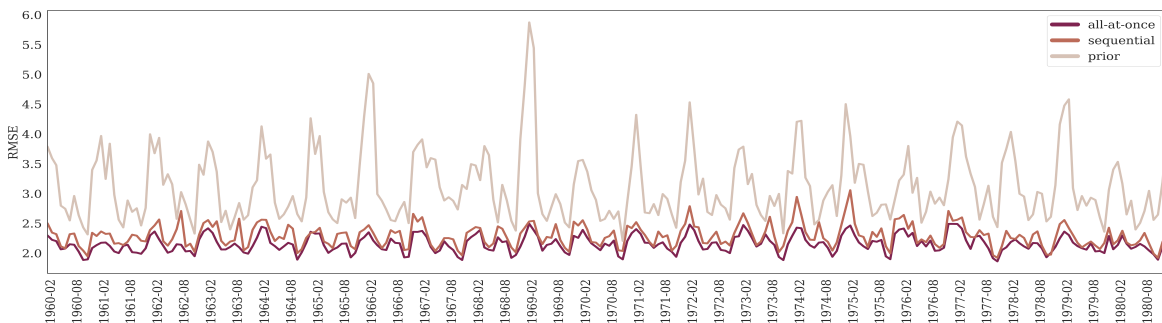
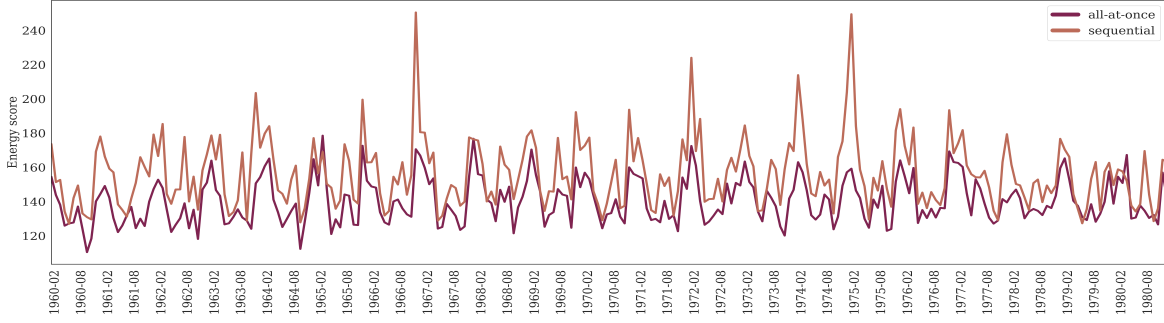


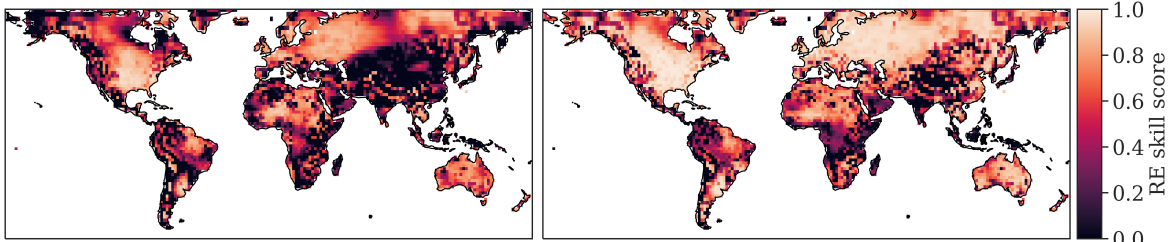
Figure 10: RMSE of the reconstruction for different assimilation schemes.

Apart from the above metrics, one can also study the spatial distribution of the RMSE skill score aggregated over the whole assimilation window (Figure 12). In this figure, negative values of the score (reconstruction poorer than background) are clamped at 0.



(a) Energy score

Figure 11: Energy score for different assimilation schemes.



(a) sequential

(b) all-at-once

Figure 12: RMSE skill scores for reconstruction of the reference dataset over the 1960-1980 period.

Figure 12 is in line with the previous results, confirming that all-at-once outperforms sequential assimilation. We see that all-at-once assimilation is able to enhance the results of sequential assimilation in regions close to available observations (see Figure 9), while performing poorly in regions where sequential assimilation also struggles. This seems to indicate that all-at-once assimilation is able to better handle spatial correlations.

5 Conclusion

Leveraging modern distributed computing techniques provided by the DASK Python library, we are able to overcome the memory bottlenecks of Ensemble Kalman Filtering and provide a distributed implementation of the Ensemble Square Root Filter that allows for non-sequential data assimilation in problems of realistic sizes. We provide comparisons of our non-sequential, all-at-once assimilation scheme with the traditional sequential one on a synthetic assimilation problem and on a real-world paleoclimatic reconstruction task. Our benchmark shows that all-at-once assimilation outperforms sequential assimilation in both situations. In passing, we also provide an assessment of the dependence of sequential assimilation on observation ordering.

By allowing for non-sequential assimilation, our framework solves the long-standing problem of having to resort to inconsistent update equations in ensemble Kalman filtering and allows for a systematic study of the effects of inconsistent updates on assimilation results. Furthermore, we believe that distributed computing opens new venues of research in data assimilation and hope that our work can serve as a first paving stone in that direction. Among the next challenges that can be tackled using our distributed assimilation framework, we believe that the development of new covariance estimation techniques is the most promising one. Indeed, our implementation makes the full state covariance matrix available to the user, as well as a compressed representation of it through its truncated SVD, thereby allowing for the implementation of complex localization techniques in a large-scale setting.

Open Research Section

Climate simulations used for the starting ensemble in the paleoclimatic reconstruction example of section 4.2 is available online at [32]. Assimilated station data is available at [36].

Acknowledgments

C. T. acknowledges funding from the Swiss National Science Foundation under project nr. 178858. S.B., J.F. and C.T. acknowledge funding from the European Commission under Horizon 2020 (ERC grant 787574). The authors would also like to thank Veronika Valler for participating in preliminary developments, Lorenz Hilfiker for helpful comments on a draft of this article and Alberto Terranova for testing the assimilation code.

References

- [1] J. L. Anderson and S. L. Anderson. A monte carlo implementation of the nonlinear filtering problem to produce ensemble assimilations and forecasts. *Monthly Weather Review*, 127(12):2741 – 2758, 1999. doi: 10.1175/1520-0493(1999)127<2741:AMCIOT>2.0.CO;2. URL https://journals.ametsoc.org/view/journals/mwre/127/12/1520-0493_1999_127_2741_amciot_2.0.co_2.xml.
- [2] J. Bhend, J. Franke, D. Folini, M. Wild, and S. Brönnimann. An ensemble-based approach to climate reconstructions. *Climate of the Past*, 8(3):963–976, 2012. doi: 10.5194/cp-8-963-2012. URL <https://cp.copernicus.org/articles/8/963/2012/>.
- [3] M. B. Bjerregård, J. K. Møller, and H. Madsen. An introduction to multivariate probabilistic forecast evaluation. *Energy and AI*, 4:100058, 2021. ISSN 2666-5468. doi: <https://doi.org/10.1016/j.egyai.2021.100058>. URL <https://www.sciencedirect.com/science/article/pii/S2666546821000124>.
- [4] S. D. Bopardikar. Randomized matrix factorization for kalman filtering. In *2017 American Control Conference (ACC)*, pages 5795–5800, 2017. doi: 10.23919/ACC.2017.7963858.
- [5] G. Burgers, P. J. van Leeuwen, and G. Evensen. Analysis scheme in the ensemble kalman filter. *Monthly Weather Review*, 126(6):1719 – 1724, 1998. doi: 10.1175/1520-0493(1998)126<1719:ASITEK>2.0.CO;2. URL https://journals.ametsoc.org/view/journals/mwre/126/6/1520-0493_1998_126_1719_asitek_2.0.co_2.xml.
- [6] G. P. Compo, J. S. Whitaker, P. D. Sardeshmukh, N. Matsui, R. J. Allan, X. Yin, B. E. Gleason, R. S. Vose, G. Rutledge, P. Bessemoulin, S. Brönnimann, M. Brunet, R. I. Crouthamel, A. N. Grant, P. Y. Groisman, P. D. Jones, M. C. Kruk, A. C. Kruger, G. J. Marshall, M. Maugeri, H. Y. Mok, Ø. Nordli, T. F. Ross, R. M. Trigo, X. L. Wang, S. D. Woodruff, and S. J. Worley. The twentieth century reanalysis project. *Quarterly Journal of the Royal Meteorological Society*, 137(654):1–28, 2011. doi: <https://doi.org/10.1002/qj.776>. URL <https://rmets.onlinelibrary.wiley.com/doi/abs/10.1002/qj.776>.
- [7] E. R. Cook, K. R. Briffa, and P. D. Jones. Spatial regression methods in dendroclimatology: A review and comparison of two techniques. *International Journal of Climatology*, 14(4):379–402, 1994. doi: <https://doi.org/10.1002/joc.3370140404>. URL <https://rmets.onlinelibrary.wiley.com/doi/abs/10.1002/joc.3370140404>.
- [8] Dask Development Team. *Dask: Library for dynamic task scheduling*, 2016. URL <https://dask.org>.
- [9] B. Efron and C. Morris. Multivariate empirical bayes and estimation of covariance matrices. *The Annals of Statistics*, 4(1):22–32, 1976. ISSN 00905364. URL <http://www.jstor.org/stable/2957992>.
- [10] G. Evensen. Sequential data assimilation with a nonlinear quasi-geostrophic model using monte carlo methods to forecast error statistics. *Journal of Geophysical Research: Oceans*, 99(C5):10143–10162, 1994. doi: <https://doi.org/10.1029/94JC00572>. URL <https://agupubs.onlinelibrary.wiley.com/doi/abs/10.1029/94JC00572>.
- [11] G. Evensen. The ensemble kalman filter: Theoretical formulation and practical implementation. *Ocean dynamics*, 53(4):343–367, 2003.
- [12] G. Evensen et al. *Data assimilation: the ensemble Kalman filter*, volume 2. Springer, 2009.
- [13] A. Farchi and M. Bocquet. On the efficiency of covariance localisation of the ensemble kalman filter using augmented ensembles. *Frontiers in Applied Mathematics and Statistics*, 5, 02 2019. doi: 10.3389/fams.2019.00003.
- [14] J. Franke, S. Brönnimann, J. Bhend, and Y. Brugnara. A monthly global paleo-reanalysis of the atmosphere from 1600 to 2005 for studying past climatic variations. *Scientific Data*, 4(1):170076, Jun 2017. ISSN 2052-4463. doi: 10.1038/sdata.2017.76. URL <https://doi.org/10.1038/sdata.2017.76>.

-
- [15] R. Furrer and T. Bengtsson. Estimation of high-dimensional prior and posterior covariance matrices in kalman filter variants. *Journal of Multivariate Analysis*, 98(2):227–255, 2007. ISSN 0047-259X. doi: <https://doi.org/10.1016/j.jmva.2006.08.003>. URL <https://www.sciencedirect.com/science/article/pii/S0047259X06001187>.
- [16] A. Gelb et al. *Applied optimal estimation*. MIT press, 1974.
- [17] T. Gneiting and A. E. Raftery. Strictly proper scoring rules, prediction, and estimation. *Journal of the American Statistical Association*, 102(477):359–378, 2007. doi: 10.1198/016214506000001437. URL <https://doi.org/10.1198/016214506000001437>.
- [18] T. Gneiting, L. I. Stanberry, E. P. Grimit, L. Held, and N. A. Johnson. Assessing probabilistic forecasts of multivariate quantities, with an application to ensemble predictions of surface winds. *TEST*, 17(2):211–235, Aug 2008. ISSN 1863-8260. doi: 10.1007/s11749-008-0114-x. URL <https://doi.org/10.1007/s11749-008-0114-x>.
- [19] I. Grooms. A comparison of nonlinear extensions to the ensemble kalman filter: Gaussian anamorphosis and two-step ensemble filters. *Computational Geosciences*, 26(3):633–650, 2022.
- [20] L. R. Haff. Empirical Bayes Estimation of the Multivariate Normal Covariance Matrix. *The Annals of Statistics*, 8(3):586 – 597, 1980. doi: 10.1214/aos/1176345010. URL <https://doi.org/10.1214/aos/1176345010>.
- [21] N. Halko, P.-G. Martinsson, and J. A. Tropp. Finding structure with randomness: Probabilistic algorithms for constructing approximate matrix decompositions. *SIAM review*, 53(2):217–288, 2011.
- [22] T. M. Hamill, J. S. Whitaker, and C. Snyder. Distance-dependent filtering of background error covariance estimates in an ensemble kalman filter. *Monthly Weather Review*, 129(11):2776 – 2790, 2001. doi: 10.1175/1520-0493(2001)129<2776:DDFOBE>2.0.CO;2. URL https://journals.ametsoc.org/view/journals/mwre/129/11/1520-0493_2001_129_2776_ddfobe_2.0.co_2.xml.
- [23] I. Harris, T. J. Osborn, P. Jones, and D. Lister. Version 4 of the cru ts monthly high-resolution gridded multivariate climate dataset. *Scientific Data*, 7(1):109, Apr 2020. ISSN 2052-4463. doi: 10.1038/s41597-020-0453-3. URL <https://doi.org/10.1038/s41597-020-0453-3>.
- [24] P. L. Houtekamer and H. L. Mitchell. A sequential ensemble kalman filter for atmospheric data assimilation. *Monthly Weather Review*, 129(1):123 – 137, 2001. doi: 10.1175/1520-0493(2001)129<0123:ASEKFF>2.0.CO;2. URL https://journals.ametsoc.org/view/journals/mwre/129/1/1520-0493_2001_129_0123_asekff_2.0.co_2.xml.
- [25] P. L. Houtekamer and F. Zhang. Review of the ensemble kalman filter for atmospheric data assimilation. *Monthly Weather Review*, 144(12):4489 – 4532, 2016. doi: <https://doi.org/10.1175/MWR-D-15-0440.1>. URL <https://journals.ametsoc.org/view/journals/mwre/144/12/mwr-d-15-0440.1.xml>.
- [26] A. Jordan, F. Krüger, and S. Lerch. Evaluating probabilistic forecasts with scoringrules. *Journal of Statistical Software*, 90(12):1–37, 2019. doi: 10.18637/jss.v090.i12. URL <https://www.jstatsoft.org/index.php/jss/article/view/v090i12>.
- [27] S. J. Julier and J. K. Uhlmann. New extension of the kalman filter to nonlinear systems. In *Signal processing, sensor fusion, and target recognition VI*, volume 3068, pages 182–193. Spie, 1997.
- [28] M. Katzfuss, J. R. Stroud, and C. K. Wikle. Understanding the ensemble kalman filter. *The American Statistician*, 70(4):350–357, 2016. doi: 10.1080/00031305.2016.1141709. URL <https://doi.org/10.1080/00031305.2016.1141709>.
- [29] O. Ledoit and M. Wolf. A well-conditioned estimator for large-dimensional covariance matrices. *Journal of Multivariate Analysis*, 88(2):365–411, 2004. ISSN 0047-259X. doi: [https://doi.org/10.1016/S0047-259X\(03\)00096-4](https://doi.org/10.1016/S0047-259X(03)00096-4). URL <https://www.sciencedirect.com/science/article/pii/S0047259X03000964>.
- [30] O. Ledoit and M. Wolf. Nonlinear shrinkage estimation of large-dimensional covariance matrices. *The Annals of Statistics*, 40(2):1024 – 1060, 2012. doi: 10.1214/12-AOS989. URL <https://doi.org/10.1214/12-AOS989>.
- [31] T. Lefebvre, H. Bruyninckx, and J. De Schutter. Kalman filters for non-linear systems: a comparison of performance. *International journal of Control*, 77(7):639–653, 2004.
- [32] Max Planck Institute for Meteorology (MPI-M). Input for ekf400: Original echem simulations (ccc400) and assimilated observations, 2017. URL <http://hdl.handle.net/21.14106/0bb12ac5cde477d3f382d9440e29d718e0943257>.

- [33] A. H. Murphy and E. S. Epstein. Skill scores and correlation coefficients in model verification. *Monthly Weather Review*, 117(3):572 – 582, 1989. doi: [https://doi.org/10.1175/1520-0493\(1989\)117\(0572:SSACCI\)2.0.CO;2](https://doi.org/10.1175/1520-0493(1989)117(0572:SSACCI)2.0.CO;2). URL https://journals.ametsoc.org/view/journals/mwre/117/3/1520-0493_1989_117_0572_ssacci_2_0_co_2.xml.
- [34] L. Nerger. On serial observation processing in localized ensemble kalman filters. *Monthly Weather Review*, 143(5):1554 – 1567, 2015. doi: 10.1175/MWR-D-14-00182.1. URL <https://journals.ametsoc.org/view/journals/mwre/143/5/mwr-d-14-00182.1.xml>.
- [35] C. E. Rasmussen and C. K. I. Williams. *Gaussian Processes for Machine Learning*. Adaptive computation and machine learning. MIT Press, 2006.
- [36] J. J. Rennie, J. H. Lawrimore, B. E. Gleason, P. W. Thorne, C. P. Morice, M. J. Menne, C. N. Williams, W. G. de Almeida, J. Christy, M. Flannery, M. Ishihara, K. Kamiguchi, A. M. G. Klein-Tank, A. Mhanda, D. H. Lister, V. Razuvaev, M. Renom, M. Rusticucci, J. Tandy, S. J. Worley, V. Venema, W. Angel, M. Brunet, B. Dattore, H. Diamond, M. A. Lazzara, F. Le Blancq, J. Luterbacher, H. Mächel, J. Revadekar, R. S. Vose, and X. Yin. The international surface temperature initiative global land surface databank: monthly temperature data release description and methods. *Geoscience Data Journal*, 1(2):75–102, 2014. doi: <https://doi.org/10.1002/gdj3.8>. URL <https://rmets.onlinelibrary.wiley.com/doi/abs/10.1002/gdj3.8>.
- [37] M. Rocklin. Dask: Parallel computation with blocked algorithms and task scheduling. In K. Huff and J. Bergstra, editors, *Proceedings of the 14th Python in Science Conference*, pages 130 – 136, 2015.
- [38] E. Roeckner, G. Bäuml, L. Bonaventura, R. Brokopf, M. Esch, M. Giorgetta, S. Hagemann, I. Kirchner, L. Kornblüeh, E. Manzini, A. Rhodin, U. Schlese, U. Schulzweida, and A. Tompkins. The atmospheric general circulation model echam 5. part i: model description. *Report / Max Planck Institute for Meteorology*, 349, 01 2003.
- [39] L. C. Slivinski, G. P. Compo, J. S. Whitaker, P. D. Sardeshmukh, B. S. Giese, C. McColl, R. Allan, X. Yin, R. Vose, H. Titchner, J. Kennedy, L. J. Spencer, L. Ashcroft, S. Brönnimann, M. Brunet, D. Camuffo, R. Cornes, T. A. Cram, R. Crouthamel, F. Domínguez-Castro, J. E. Freeman, J. Gergis, E. Hawkins, P. D. Jones, S. Jourdain, A. Kaplan, H. Kubota, F. L. Blancq, T.-C. Lee, A. Lorrey, J. Luterbacher, M. Maugeri, C. J. Mock, G. K. Moore, R. Przybylak, C. Pudmenzky, C. Reason, V. C. Slonosky, C. A. Smith, B. Tinz, B. Trewin, M. A. Valente, X. L. Wang, C. Wilkinson, K. Wood, and P. Wyszynski. Towards a more reliable historical reanalysis: Improvements for version 3 of the twentieth century reanalysis system. *Quarterly Journal of the Royal Meteorological Society*, 145(724):2876–2908, 2019. doi: <https://doi.org/10.1002/qj.3598>. URL <https://rmets.onlinelibrary.wiley.com/doi/abs/10.1002/qj.3598>.
- [40] C. Snyder. Introduction to the Kalman filter. In *Advanced Data Assimilation for Geosciences: Lecture Notes of the Les Houches School of Physics: Special Issue, June 2012*. Oxford University Press, 10 2014. ISBN 9780198723844. doi: 10.1093/acprof:oso/9780198723844.003.0003. URL <https://doi.org/10.1093/acprof:oso/9780198723844.003.0003>.
- [41] M. K. Tippett, J. L. Anderson, C. H. Bishop, T. M. Hamill, and J. S. Whitaker. Ensemble square root filters. *Monthly weather review*, 131(7):1485–1490, 2003.
- [42] C. Travetletti, D. Ginsbourger, and N. Linde. Uncertainty quantification and experimental design for large-scale linear inverse problems under gaussian process priors. *SIAM/ASA Journal on Uncertainty Quantification*, 11(1):168–198, 2023. doi: 10.1137/21M1445028. URL <https://doi.org/10.1137/21M1445028>.
- [43] V. Valler, J. Franke, and S. Brönnimann. Impact of different estimations of the background-error covariance matrix on climate reconstructions based on data assimilation. *Climate of the Past*, 15(4):1427–1441, 2019. doi: 10.5194/cp-15-1427-2019. URL <https://cp.copernicus.org/articles/15/1427/2019/>.
- [44] E. A. Wan and R. Van Der Merwe. The unscented kalman filter for nonlinear estimation. In *Proceedings of the IEEE 2000 Adaptive Systems for Signal Processing, Communications, and Control Symposium (Cat. No. 00EX373)*, pages 153–158. Ieee, 2000.
- [45] G. Welch and G. Bishop. An introduction to the kalman filter. Technical Report TR95041, Department of Computer Science, University of North Carolina, Chapel Hill, 2000.
- [46] E. Wheatcroft. Interpreting the skill score form of forecast performance metrics. *International Journal of Forecasting*, 35(2):573–579, 2019. ISSN 0169-2070. doi: <https://doi.org/10.1016/j.ijforecast.2018.11.010>. URL <https://www.sciencedirect.com/science/article/pii/S0169207019300093>.
- [47] J. S. Whitaker and T. M. Hamill. Ensemble data assimilation without perturbed observations. *Monthly Weather Review*, 130(7):1913 – 1924, 2002. doi: 10.1175/1520-0493(2002)130(1913:EDAWPO)2.0.CO;2. URL https://journals.ametsoc.org/view/journals/mwre/130/7/1520-0493_2002_130_1913_edawpo_2_0_co_2.xml.

-
- [48] J. S. Whitaker, T. M. Hamill, X. Wei, Y. Song, and Z. Toth. Ensemble data assimilation with the ncep global forecast system. *Monthly Weather Review*, 136(2):463–482, 2008.
- [49] A. B. Yoo, M. A. Jette, and M. Grondona. Slurm: Simple linux utility for resource management. In D. Feitelson, L. Rudolph, and U. Schwiegelshohn, editors, *Job Scheduling Strategies for Parallel Processing*, pages 44–60, Berlin, Heidelberg, 2003. Springer Berlin Heidelberg. ISBN 978-3-540-39727-4.